

On-body to On-body Channel Characterization

Fabio Di Franco, Christos Tachtatzis, Ben Graham,
David Tracey, Nick F. Timmons and Jim Morrison

WiSAR Lab, Letterkenny Institute of Technology
Port Road, Letterkenny, Co. Donegal, Ireland

{fabio, christos, ben, david, nick, jim}@wisar.org

Abstract—Interest in on-body communication channels is growing as the use of wireless devices increases in medical, consumer and military sensor applications. This paper presents an experimental investigation and analysis of the narrowband on-body propagation channel. This analysis considers each of the factors affecting the channel during a range of stationary and motion activities in different environments with actual wireless mote devices on the body. Use of such motes allows greater freedom in the subject's movements and the inclusion of real-world indoor and outdoor environments in a test sequence. This paper identifies and analyses the effect of the different components of the signal propagation (mean propagation path gain, large-scale fading and small-scale fading) and the cause of the losses and variation due to activities, positions or environmental factors. Our results show the effect on the received signal and the impact of voluntary and involuntary movements, which cause shadowing effects. The analysis also allows us to identify sensor positions on the body that are more reliable and those positions that may require a relay or those that may be suitable for acting as a relay.

Index Terms— Channel Characterisation, channel propagation, Embedded system design, Body Area Networks

1. INTRODUCTION

Body Area Networks (BAN) have attracted significant attention in medical and consumer applications. The IEEE 802.15.6 task group is defining the physical and the data link layer for BANs. The task group identified four distinct communication scenarios between devices: implantable to implantable, implantable to on/off body, on-body to on-body and on-body to off-body [1].

This paper presents experimental results from a series of on-body tests. There have been numerous other studies of the on-body propagation channel, but the analysis presented here considers each of the factors affecting the channel individually. Fort [2] analysed the indoor signal propagation around the torso and he presented a distance based model using the results of these experiments. Miniutti [3] analysed the received signal using a series of narrowband on-body indoor channel measurements at 900 and 2400 MHz ISM bands when the subject was standing, walking and running. Cotton [4] performed extensive on-body measurements and he focused on the signal fading experienced in a wireless body area network instead of path loss. Hall [5] showed extensive on-body measurements at 2.4GHz with different antennas and in different positions of the body focusing on path gain. Reusens [6] presented a simulated and experimental on-body model of the path loss for transmitter and receiver separation of between 5 and 40cm testing different regions of the body separately and not considering the motion of the person. D'Errico [7] analyses the body channel for 2.45 GHz and 3-5

GHz using subjects performing a set of exercises on the spot while attached to test instruments in an anechoic chamber and in an indoor environment. Importantly, he also analyses the effects of slow fading, shadowing and mean channel gain during these tests. In this paper we follow a similar approach to D'Errico, but we use a different test setup with real motes, different locations on the body, different antenna. The use of real motes, which are battery-powered, means freedom in the movements and therefore a more typical scenario and also allows the inclusion of an outdoor environment in a continuous sequence of tests.

Our work experimentally characterises the on-body to on-body propagation channel between different positions on the body and interprets the results by decomposing the received signals in terms of mean path gain, large-scale fading and small-scale fading. This decomposition is useful in such a time-variant propagation channel, which is affected by human movement, device placement and the surrounding environment. This gives a better understanding of the factors affecting the channel than by considering the distance based model or the fading behaviour in isolation. It enables us to identify positions on the body that are more likely to have poor channel conditions and may require the aid of relays to maintain connectivity. We show that the distance between transmitter and receiver is not the only factor to consider when estimating the path loss. In fact the voluntary and involuntary movements always present in the stationary position [8] cause shadowing affecting the line-of-sight.

The remainder of this paper is organised as follows. The test setup, the scenario and experimental procedure are described in Section 2. Section 3 introduces the methodology used to analyse the signal propagation. Section 4 shows the results for mean path gain. Section 5 shows the results for the fading distinguishing the large-scale fading from the small-scale fading. The paper concludes in Section 6.

2. MEASUREMENT SETUP & SCENARIO

The on-body channel measurements were carried out in time domain. The test setup consists of seven Tmote-Sky motes; one as a transmitter and the other six as receivers.

The transmitter runs an application on the Contiki operating system that broadcasts a frame every 15.6ms at max output power (0dBm) and with centre frequency at 2.395GHz. This frequency is part of the new medical body area network band that is undergoing FCC approval and is outside the 2.4GHz ISM band guaranteeing no interference during the tests. The frames sent by the transmitter contain a monotonic increasing sequence number. The receiver nodes stay in receive mode for

the duration of the experiment. When frames are received correctly, their sequence number and their measured received signal strength are recorded in flash memory. When frames are lost, their corresponding sequence numbers are not present in the flash and their received signal strength is assumed to be less than the sensitivity of the Tmote-Sky radio (-95dBm).

As shown in Figure 1, the transmitter (TX) was placed on the chest of the subject while the 6 receivers (RX) were placed on: Right abdominal Side (1), right hip (2), left side of the back (Latissimus Dorsi referred to Dorsi for the remainder of this paper) (3), low centred back (4), left arm (5), left ankle (6). Care was taken to ensure that the inverted F antenna of each node was placed 2cm away from the subject's body.

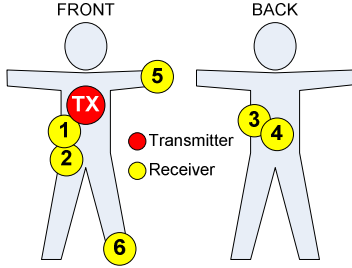


Figure 1 On-body position of TX and RX's

The subject performed typical stationary and dynamic, day-to-day activities for specified durations. The sequence consisted of indoor (sitting 15s, standing still 15s, walking 25s, running 15s) and outdoor (walking 45s, running for 25s). This sequence was repeated 3 times for validation purposes.

Table 1 shows the distance between transmitter and receiver during the different activities.

Chest (TX)	Distance between TX and RX (cm.)			
RX Position	standing	sitting	walking	running
Side (1)	23	23	23	23
Hip (2)	33	30	33	33
Dorsi (3)	35	35	35	35
Back (4)	53	53	53	53
Arm (5)	50	38	43/60	33/35
Ankle (6)	111	86	110/125	110/132

Table 1 Distance between TX and RX during different activities. For arm and ankle, which experience great movements during dynamic activities, the minimum and the maximum distance are indicated (min/max).

The stationary positions were measured at the centre of a room (9mx3mx2m) in an office building which contained desks and computers. The indoor activities were performed in a corridor (40mx4mx2.5m), while the outdoor activities used a 200m open space. The measured average walking and running speeds were 1.3m/s (2 steps per second) and 2.3m/s (2.7 steps per second) respectively. During the length of experiment, a total of 231000 samples were collected from the 6 receivers.

3. CHANNEL PROPAGATION

We analyse the envelope received signal power $P(t_n)$ as the product of three components: mean path gain G_0 , large-scale fading (or shadowing) $L(t_n)$ and small-scale fading $S(t_n)$.

$$P(t_n) = G_0 \cdot L(t_n) \cdot S(t_n) \quad (1)$$

The mean path gain G_0 is range dependent and in free-space it decreases with the square of the distance. It is dependent on the relative position of the transmitter and the

receiver, the antenna used, the distance between the antennas and the presence of line-of-sight.

The fluctuation of the signal envelope around the mean is known as fading. The large-scale fading $L(t_n)$ refers to slow fluctuation of the received signal in space and time, which is caused by shadowing effects due to obstruction from human body. Small-scale fading $S(t_n)$ refers to rapid fluctuation of the received signal in space and time and results from the constructive and destructive combination of different paths as a result of reflection, scattering, diffraction (multipath).

4. MEAN PROPAGATION PATH GAIN

The mean path gain G_0 was computed as the mean of the received signal results for each activity and position. When the mean path gain is expressed in dB, it is negative, indicating the power path loss of the transmitted signal. Figure 2 shows the mean path gain for different RX positions and different activities. It shows that the distance between TX and RX, the presence of line-of-sight and the environment are the main elements that affect the mean propagation path and in particular we can observe the following:

- Although the chest-arm distance is longer than the chest-dorsi (Table 1), the former experiences lower path loss than the latter for all the activities. This can be justified by the stronger line-of-sight of the chest-arm path.
- While sitting inside, the chest-side position experienced higher path loss than other scenarios this was caused by the shadowing of the arm.

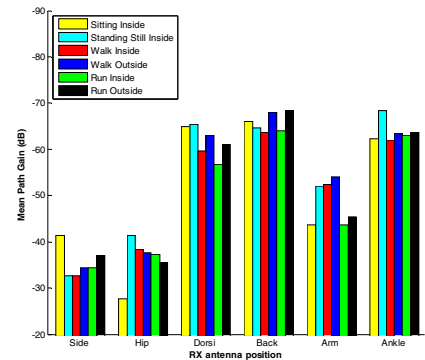


Figure 2 Mean Path Gain for different RX antenna positions and activities

- While sitting inside, the chest-hip experienced lower path loss than other scenarios due to the reduced distance and stronger line-of-sight
- The chest-dorsi and chest-back show that during dynamic activities the path loss is reduced when the subject is inside compared to outside; in fact the presence of multipath is much stronger inside than outside as shown in Section 5.2.

5. FADING RESULTS

In this paper we use the terms large-scale fading, slow fading and shadowing interchangeably to refer to the signal variation (in space and time) caused by shadowing of the human body. Similarly, we use small-scale fading and fast fading interchangeably to refer to the rapid fluctuations of the received signal. We compute the fading $F(t_n) = P(t_n)/G_0$ where $F(t_n) = S(t_n)L(t_n)$ from equation 1.

5.1. Large-scale Fading

In order to distinguish the large-scale fading $L(t_n)$ from the total fading we apply a moving average function to $F(t_n)$. The window size of the moving average was selected so as the variations from multipath are smoothed out while significant variations of shadowing are still present. Taking into consideration the speed that the subject moves (370 ms per step on running activities) the window size was selected to be 156 ms which is equivalent to number of sample $W=10$.

$$L(t_n) = \frac{1}{W} \sum_{n-\frac{W}{2}}^{n+\frac{W}{2}} \frac{P(t_n)}{G_0} \quad (2)$$

Figure 3 shows the large-scale fading $L(t_n)$ for all activities and positions. While stationary, the large scale fading effect is present due to involuntary movements [8]. Furthermore, the large-scale fading for chest-dorsi is higher than chest-hip for stationary activities, as the line-of-sight was obstructed. This made it more sensitive to small movements and so involuntary movement caused large variation in the received signal.

We have also shown the chest/ankle position experienced higher standard deviation during walking compared to running; in line with the results reported by D'Errico [7] for the position hip to foot. Our results for indoors also validate those of [7] although our subject was moving along a corridor and not on the spot and so experiencing more typical movement during the tests and longer duration of the each activity.

The results presented in Figure 3 show how a link is affected by the shadowing with respect to another link. To understand the variation over time of the large scale fading between nodes during particular activities, the cross-correlation coefficients of the large-scale fading results were determined and are shown in Table 2 for the case of running outside. For example right side and right hip have a high positive correlation as both suffer from shadowing at the same time, while the right side and left ankle have high negative correlation indicating that when one suffers high large-scale fading the other has low large-scale fading. This is due to the alternating movements of arms and legs when running. Other dynamic activities show similar results.

The cross correlation shown Table 2 would be useful to select the appropriate position for nodes that act as relays. Such use of relays in BANs has been proposed in the restricted tree topology of the 802.15.6 draft [9].

5.2. Small-scale Fading

The instantaneous received signal strength is a sum of many components coming from different directions due to the many reflections of the transmitted signal reaching the receiver. If each component has the same amplitude and its phase is uniformly distributed in the range $[0, 2\pi]$, the amplitude of the received signal obeys a Rayleigh distribution. However, if a dominant component is present as in the case of line-of-sight path, the received signal obeys a Rice distribution. The Ricean K -factor is defined as the ratio of the power in the line-of-sight component to the power in the diffuse component. The diffuse component consists of the energy that is diffracted, reflected, scattered from the body or the surrounding environment [2][8]. When $K \rightarrow 0$, the Rice

distribution approximates the Rayleigh distribution; when $K \rightarrow \infty$, the Rice distribution approximates the Gaussian distribution.

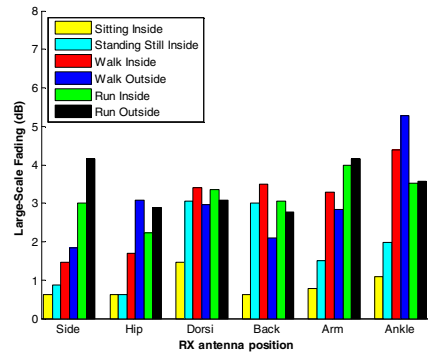


Figure 3 Large-Scale Fading for different RX antenna positions and activities.

Running outside TX = Chest	Right Side abdominal (1)	right hip (2)	Right dorsi (3)	low back (4)	left arm (5)	left ankle (6)
Right Side abdominal (1)	1.00	0.69	-0.27	0.21	0.44	-0.61
right hip (2)	0.69	1.00	-0.21	0.20	0.46	-0.66
Right dorsi (3)	-0.27	-0.21	1.00	0.06	-0.23	0.22
low back (4)	0.21	0.20	0.06	1.00	-0.08	-0.17
left arm (5)	0.44	0.46	-0.23	-0.08	1.00	-0.51
left ankle (6)	-0.61	-0.66	0.22	-0.17	-0.51	1.00

Table 2 Cross-Correlation Coefficient of Large-Scale fading while running outside

In this paper, the small-scale fading $S(t_n)$ is calculated as the ratio between the received signal $P(t_n)$ and the product between the mean propagation path gain G_0 and the large scale fading $L(t_n)$.

$$S(t_n) = \frac{P(t_n)}{G_0 \cdot L(t_n)} = \frac{F(t_n)}{L(t_n)} \quad (3)$$

The statistical analysis of the small-scale fading was performed by attempting to fit seven commonly used probability distributions to the small-scale fading experimental data, using the maximum likelihood estimates function in Matlab. Subsequently, the second order Akaike Information Criteria (AIC) [2] has been used to choose the best distribution fit among the seven with minimum loss of information.

The AIC reveals that the Rice distribution is the best fit to our experimental small-scale fading data, due to the presence of a line-of-sight and multipath for the diffuse component. Table 3 shows the Ricean K -factor across different activities and position on the body. A high K -factor indicates high ratio of line-of-sight component over multi-path in the received power. When the subject is stationary, it is expected that K -factor will be very high because the subject is stationary and consequently the small scale-fading is low, as shown in Table 3. As expected, the K -factor is lower when the subject is moving inside (due to strong multi-path contribution). In fact, for any of the on-body receivers, the K -factor is generally lower when walking inside compared to outside. In particular, the channel chest to left ankle presents the lowest K -factor indicating no line-of-sight, whereas the chest to right side channel is the most stable (higher K -factor) indicating a strong line-of-sight. The dorsi position for all the dynamic scenarios presents a low K -factor.

TX = Chest	Ricean K factor					
	Standing	Sitting	Walking Inside	Walking Outside	Running Inside	Running Outside
Right Side abdominal (1)	101	592	25	42	0.1	5.7
right hip (2)	720	56	30	32	12	12
Right dorsi (3)	85	348	0.5	0.8	0.01	1.4
low back (4)	16	296	1	5.8	0.02	1.5
left arm (5)	63	432	2	5.2	2.2	6.7
left ankle (6)	271	172	0.9	1.5	0.01	0.3

Table 3 Ricean K-factor for different RX positions and activities

The Level Crossing Rate and Average Fade Duration can be used to quantify the rate and duration of small-scale fading dips. The Level Crossing rate (indicated in Hz) indicates the number of positive crossings per second with respect to a given threshold. The Average Fade Duration is the total time that a signal remains below that threshold over the number of crossings. Figure 4 shows LCR and AFD for the low back position for thresholds from -20dB to 0dB. Considering an assigned 10 dB threshold, the LCR was 3Hz when running inside and 2.4Hz when walking inside. The LCR is reduced to 2.4Hz when running outside and 0.3Hz when walking outside. Figure 4 also shows that the AFD is similar for all the activities; the AFD is also very limited for the threshold of 10 dB (only 16ms) indicating that the signal remains under that threshold only for the duration of a single frame, as frames were transmitted every 15.6ms.

The higher LCR in the case of activities performed inside is due to the multipath. When the subject is stationary, the low-value of LCR indicates that the channel is stable.

6. CONCLUSION

We have focused on the mean propagation gain and signal fading experienced by a wireless body area network consisting of a number of strategically placed body-worn receivers operating at 2.395 GHz for a subject staying in two different physical environments (inside and outside) and performing six different activities. Based on time-synchronous measurements, it has been established that the mean path and local environment play an important role in the determination of on-body propagation characteristics.

Our results have also emphasised that the distance between transmitter and receiver is not the only main factor to consider when estimating the path loss for on-body channels during activities; in fact, the path loss is mainly influenced by the presence of a direct line-of sight and body movements can break this line-of sight generating large-scale fading. We also showed the shadowing correlation for large-scale fading that could be used to identify a good position for a relaying node to act for a particular relayed node, such as occurs when those 2 nodes are correlated negatively during an activity.

The Level Crossing Rate and Average Fade Duration were shown and they indicate that indoor activities suffer higher small-scale fading than outdoor activities as expected due to the elevated multi-path.

Furthermore, the use of real motes, that sample and store signal strength every 15.6 ms, has allowed us to determine the stability and characteristics of the channel over a relatively long period of time. Furthermore, this shows that a mote can potentially both react quickly enough to channel conditions and use past trends to adjust its performance to overcome

adverse and time variant channel conditions. Further work to develop algorithms using this stored data is planned.

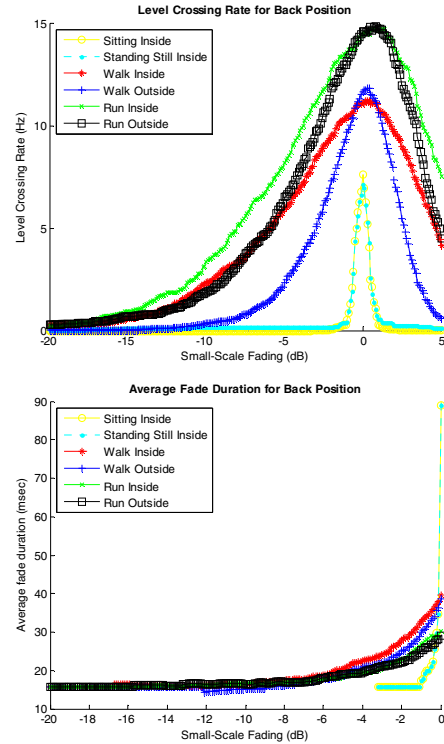


Figure 4 Level Crossing Rate, Average Fade Duration of Small-Scale Fading

ACKNOWLEDGMENT

This work was funded by Enterprise Ireland ARE program.

REFERENCES

- [1] K. Y. Yazdandoost, K. Sayrafian, "Channel Model for Body Area Network (BAN)", IEEE P802.15-08-0780-09-0006, <https://mentor.ieee.org/802.15/dcn/08/15-08-0780-09-0006-tg6-channel-model.pdf>
- [2] Fort, A.; Desset, C.; Wambacq, P.; Biesen, L.V.; "Indoor body-area channel model for narrowband communications," *Microwaves, Antennas & Propagation, IET*, vol.1, no.6, pp.1197-1203, Dec. 2007
- [3] D. Miniutti, L. Hanlen, D. Smith, A. Zhang, D. Lewis, D. Rodda, B. Gilbert, "Narrowband Channel Characterization for Body Area Networks", IEEE P802.15-08-0421-00-0006, <https://mentor.ieee.org/802.15/dcn/08/15-08-0421-00-0006-narrowband-channel-characterization-for-ban.pdf>
- [4] Cotton, S.L.; Scanlon, W.G.; "An experimental investigation into the influence of user state and environment on fading characteristics in wireless body area networks at 2.45 GHz," *Wireless Communications, IEEE Transactions on*, vol.8, no.1, pp.6-12, Jan. 2009
- [5] Hall, P.S.; Yang Hao; Nechayev, Y.I et al, "Antennas and Propagation for On-Body Communication Systems," *Antennas and Propagation Magazine, IEEE*, vol.49, no.3, pp.41-58, June 2007
- [6] E. Reusens, W. Joseph, B. Latre, et al, "IEEE Characterization of On-Body Communication Channel and Energy Efficient Topology Design for Wireless Body Area Networks", *Information Technology in Biomedicine, IEEE Transactions on*, vol.13, no.6, pp.933-945, Nov. 2009
- [7] D'Errico, Ouvry, "A Statistical Model for On-Body Dynamic Channel", *Int J Wireless Inf Networks*, Springer
- [8] F. Di Franco, C. Tachtatzis, B. Graham, M. Bykowski, D. C. Tracey, N.F. Timmons, J. Morrison "The effect of body shape and gender on Wireless Body Area Network", 1st Middle East Conference on Antennas and Propagation, Oct 2010
- [9] Arthur Astrin et al. "TG6 Draft", IEEE P802.15-10-0245-06-0006